A Solar Chimney for renewable energy production: thermo-fluid dynamic optimization by CFD analyses

IOP Conf. Series: Journal of Physics: Conf. Series **923** (2017) 012047 doi:10.1088/1742-6596/923/1/012047

A Solar Chimney for renewable energy production: thermo-fluid dynamic optimization by CFD analyses

S Montelpare[1], V D'Alessandro[2], A Zoppi[2] and E Costanzo[2]

[1] University "G. d'Annunzio" of Chieti-Pescara, Engineering and Geology Department (INGEO)
Viale Pindaro 42, 65127 Pescara (Italy)
[2] Marche Polytechnic University, Industrial Engineering and Mathematical Sciences Department (DIISM)
Via Brecce Bianche 1, 60131 Ancona (Italy)

E-mail: s.montelpare@unich.it

Abstract. This paper analyzes the performance of a solar tower designed for renewable energy production. The Solar Chimney Power Plant (SCPP) involves technology that converts solar energy by means of three basic components: a large circular solar collector, a high tower in the center of the collector and a turbine generator inside the chimney. SCPPs are characterized by long term operational life, low maintenance costs, zero use of fuels, no use of water and no emissions of greenhouse gases. The main problem of this technology is the low energy global conversion coefficient due to the presence of four conversions: solar radiation > thermal energy > kinetic energy > mechanical energy > electric energy. This paper defines its starting point from the well known power plant of Manzanares in order to calibrate a numerical model based on finite volumes. Following that, a solar tower with reduced dimensions was designed and an analysis on various geometric parameters was conducted: on the inlet section, on the collector slope, and on the fillet radius among the SUPP sections. Once the optimal solution was identified, a curved deflectors able to induce a flow swirl along the vertical tower axis was designed.

1. Introduction

The demand for energy has significantly increased in the last decades and, as a direct consequence, the use of fossil fuels, deforestation and increased air pollution are contributing to the exponential growth of greenhouse gases. These are the main causes of global warming and of the recent climatic changes. In this scenario there is a growing need for new technologies able to produce electricity with renewable sources. Solar energy is one of these and many people consider it the main resource for the future.

The Solar Chimney Power Plant (SCPP) or Solar Updraft Power Plant (SUPP) is a technology that combines solar and wind energies in order to produce electricity by means of a turbine. The power plant is composed of three main components: a very large collector operating as a greenhouse, a high tower allowing the updraft movement of the warmer air and a wind turbine placed at the base of the tower and elaborating the ascending flow. These systems are characterized by a very long operational life, poor maintenance costs, the absence of fossil

fuels, the absence of water consumption and no greenhouse gases emissions. Thanks to this easy technology this kind of power plant is normally realized with economic and locally accessible materials. The main disadvantage of the SUPP is its very low efficiency due to the high number of energy conversions with multiple η: solar radiation $\rightarrow$ air heating $\rightarrow$ air movement $\rightarrow$ turbine rotation $\rightarrow$ electric production.

The first experimental prototype was realized in 1982 by Prof. Schlaich with his colleagues in Manzanares (Spain), as a result of a joint venture between the German government and a Spanish utility. The pilot prototype had a 194.6 $[m]$ high tower with a diameter of 10 $[m]$ and a collector with a radius of 122 $[m]$. The collector roof was mainly realized in plastic with the inner glass part connecting to the tower. The collector height was about 1.85 $[m]$ above ground. The air temperature increase in the collector was measured up to 17 $[^{\circ}C]$ and the air velocity upcoming to the turbine was 12 $[m/s]$. The turbine had four blades and was arranged in a vertical axis configuration at the base of the tower [1, 2]. The prototype operated with a peak power of about 50 $[kW]$ for seven years from 1983 to 1989 [3].

The Manzanares project launched the start of a series of research works aimed at evaluating the energy potential of SUPP systems all around the world. A full literature review is reported by Zhou et al. [4, 5], by Dhahri and Omri [6], and by Hussain H. Al-Kayiem et al. [7]. Pasumarthi and Sherif [8, 9] studied the performance of a small-scale physical prototype and concluded that an intermediate absorber in the collector had the potential to boost mass flow rate. Gannon and von Backström [10] introduced a thermodynamic cycle approach with an isobaric collector model and analyzed the energy conversion processes with a temperature-entropy diagram of the air standard cycle also considering system losses (Fig.2). Bernardes et al. [11] and Pretorius and Kröger [12] developed more comprehensive analytic collector steady-state models using the Boussinesq approximation to calculate the density. Von Backström and Gannon analyzed turbine performance in a SUPP with radial inflow through inlet guide vanes at the base of the chimney [13]. Schlaich et al., [14] studied a water-filled system placed on the ground under the collector roof as an additional cheap and effective heat storage system. Cottam [15] analyzed the role of the exponential canopy profile shape in power output, and concluded that an exponential canopy with a collector constant cross-sectional flow area produces the greatest power output. Sangi et al. [16] described an analytic model for the SUPP starting from Navier-Stokes equations and validated their findings with respect to a CFD model by also considering the ground heat storage. Fasel [17] numerically investigated the SUPP with unsteady RANS calculations by using ANSYS Fluent and an in-house developed Computational Fluid Dynamics (CFD) code, confirming that the output power follows the cubic scaling predicted by theory. Koonsrisuk and Chitsomboon [18] used CFD technology to investigate the changes in flow properties caused by the variations of flow area.

This paper shows the results of analyses carried out on a SUPP having a reduced dimension with respect to Manzanares (Fig.1); i.e. a tower height of 60 $[m]$ with a diameter of 4 $[m]$ and a collector with a 60 $[m]$ radius. The choice to analyze a different model is related to the advantages of using small dimensions both for numerical and experimental approaches.

2. Thermodynamic Cycle

As shown by Gannon [10], it is possible to analyze the SUPP as an ideal air standard cycle similar to a gas turbine one (Fig.2). Assuming that all components are ideal and that all processes are loss free, the aim was to find a relationship between the plant performance and variables such as chimney height and collector temperature increase.

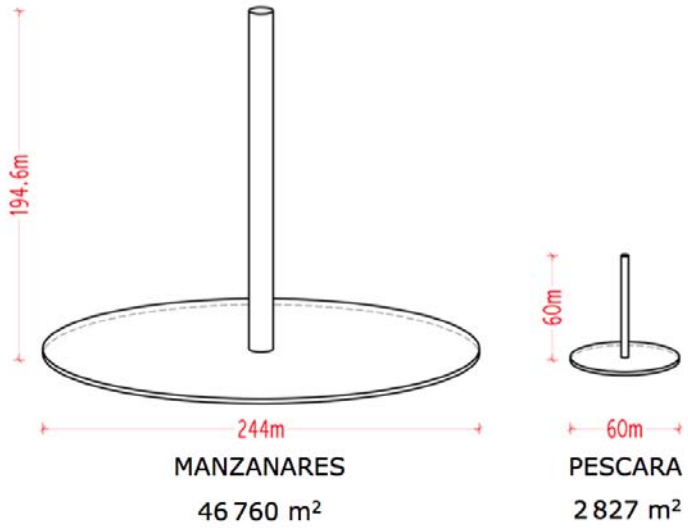

Figure 1: Scaled model.

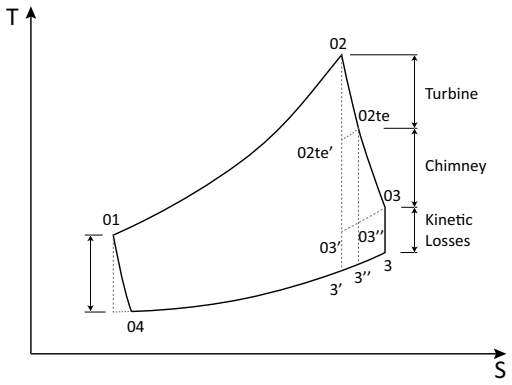

Figure 2: SUPP Thermodynamic air cycle.

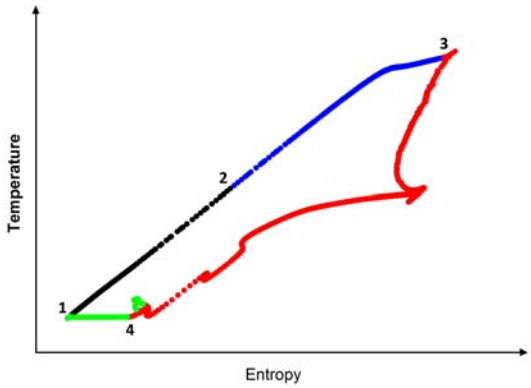

Figure 3: CFD SUPP Thermodynamic cycle.

The process fluid (air) gains heat and so does enthalpy inside the collector (phase $1 \rightarrow 2$) due to the convective exchanges with the roof's internal surface and the absorber upper surface. Kinematic losses related to the collector inlet flow and to the collector-tower junction are normally disregarded in the literature thermodynamic analyses, but actually they significantly modify the available energy of flow that should be converted downstream in turbine and that is instead converted in entropy. Point 2 corresponds to the vertical axis turbine inlet at the base of the chimney tower; the power extracted in the section $02 \rightarrow 02_{te}$ corresponds only to pressure and temperature variations, because of a constant cross sectional area corresponds to same velocities upstream and downstream the turbine. For this reason some authors do not agree with the use of the Betz theory, that is instead largely used in the SUPP analyses; in fact, this paper does not consider the Betz limit suitable. The section $02_{te} \rightarrow 3$ corresponds to the negative gravitational work $g/\Delta z$ plus the friction losses up to the chimney exit and to the kinetic losses of the flow leaving the SUPP. The $3 \rightarrow 4$ and $4 \rightarrow 1$ phases correspond to the fluid loop external to the SUPP.

The cycle efficiency may be expressed as:

$$\eta = \frac{\text{ShaftPowerOut}}{\text{SolarPowerIn}} \tag{1}$$

The energy exchanges in the SUPP collector can be obtained by using the thermodynamic first law for flowing fluid:

$$\dot{Q} - \underbrace{\dot{W}'}_{=0} = \dot{m}\left[(h_{02} - h_{01}) + \underbrace{\frac{v_{02}^2 - v_{01}^2}{2}}_{\ll} + \underbrace{g\,(z_{02} - z_{01})}_{\simeq 0}\right] \tag{2}$$

by assuming a constant specific heat value:

$$\dot{Q}_{solar} = \dot{m} \cdot c_p \cdot (T_{01} - T_{02}) \tag{3}$$

The power extracted by the turbine is:

$$\underbrace{\dot{Q}}_{\simeq 0} - \dot{W}_{turb} = \dot{m}\left[(h_{02,\,te} - h_{02}) + \underbrace{\frac{v_{02,\,te}^2 - v_{02}^2}{2}}_{=0} + \underbrace{g\,(z_{02,\,te} - z_{02})}_{\simeq 0}\right] \tag{4}$$

$$\dot{W}_{turb} \cong \dot{m} \cdot c_p \cdot \eta_{is,\,turb} \cdot (T_{02,\,te'} - T_{02}) \tag{5}$$

On the basis of the reported equations, the main solutions for increasing the system efficiency are:

- an increase of the turbine enthalpy drop, with a maximum limit due to a near zero mass flow [10];
- a more detailed design of the collector section in order to reduce energy losses and also to increase the turbine inlet enthalpy.

This paper focuses its attention on solutions able to reduce the kinetic losses at the inlet and outlet of the collector and on the use of a swirl flow to modify the turbine inlet velocity profile. Figure 3 shows the thermodynamic cycle along a streamline of the flow pattern; it is possible to observe a different behavior from point 3 to point 4 because the CFD model does not consider the presence of the turbine. The CFD model exhibits a simultaneous temperature and entropy increase due to the heat transfer with the tower internal surface and to the friction losses; instead, the wind turbine, that is present in the real system, extracts the mechanical work from the flow's enthalpy by inducing a temperature decrease and an entropy increase.

3. Analytic Model

The SUPP collector is the part of the system where the main heat exchanges take place and where the flow enthalpy increase occurs. Several authors have proposed more or less simplified models able to solve the temperature and pressure distributions with an iterative approach.
Figure 5 shows the equivalent electric scheme for a collector section of the analyzed model; the solar radiation **S** directly induces a temperature increase in the absorber surface and in the collector roof by way of a radiative heat exchange, while the air flow exhibits a temperature increase mainly due to the convective heat exchange with the collector internal surfaces.
For the collector roof:

$$\begin{aligned} S_R + h_{r,\,abs\to roof}\,(T_{abs} - T_{roof}) = h_{c,\,roof\to amb}\,(T_{roof} - T_{amb}) + ... \\ ...h_{r,\,roof\to sky}\,(T_{roof} - T_{sky}) + h_{c,\,roof\to air}\,(T_{roof} - T_{air}) \end{aligned} \tag{6}$$

For the absorber surface:

$$S_P = h_{r,\,abs\to roof}\,(T_{abs} - T_{roof}) + h_{k,\,abs\to ground}\,(T_{abs} - T_{ground}) + \ldots \\ \ldots + h_{c,\,abs\to air}\,(T_{abs} - T_{air}) \tag{7}$$

For the air flow:

$$\frac{\dot{m}\cdot c_p}{2\pi r}\cdot\frac{\Delta T_f}{\Delta r} = h_{c,\,roof\to air}\,(T_{roof} - T_{air}) + h_{c,\,abs\to air}\,(T_{abs} - T_{air}) \tag{8}$$

The radiative heat fluxes with the roof collector and with the absorber surface which are related to the solar radiation q_{solar} and to the glass transmission coefficient of the roof τ:

$$S_R = (1-\tau)\cdot\dot{q}_{solar} \tag{9}$$

$$S_P = \tau\cdot\dot{q}_{solar} \tag{10}$$

The radiative heat exchange coefficient may be evaluated with the subsequent relations [19]:

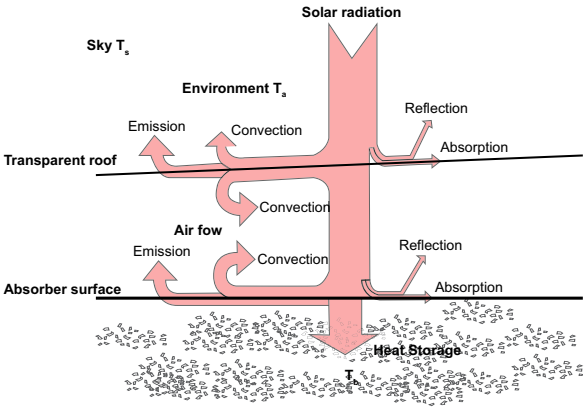

Figure 4: Collector heat fluxes.

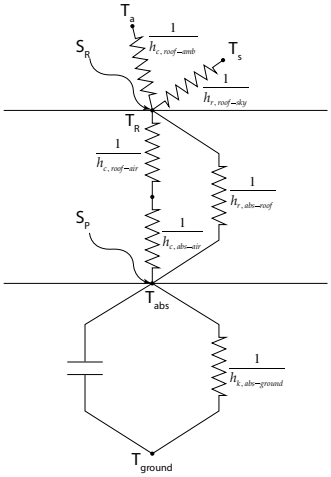

Figure 5: Collector thermal resistance network.

$$h_{r,\,roof\to sky} = \varepsilon_{roof}\cdot\sigma\cdot\left(T_{roof}^2 + T_{sky}^2\right)\cdot(T_{roof} + T_{sky}) \tag{11}$$

$$h_{r,\,abs\to roof} = \frac{1}{\frac{1}{\varepsilon_{abs}} + \frac{1}{\varepsilon_{roof}} - 1}\cdot\sigma\cdot\left(T_{abs}^2 + T_{roof}^2\right)\cdot(T_{abs} + T_{roof}) \tag{12}$$

The radiative heat exchange coefficient may be evaluated with the subsequent relations [5]:

$$h_{c,\,roof\to amb} = 5.7 + 3.8\cdot v_{wind} \tag{13}$$

$$h_{c,\,roof\to air} = \frac{\left(f/8\right)(\mathrm{Re} - 1000)\,\mathrm{Pr}}{1 + 12.7\left(f/8\right)^{1/2}\left(\mathrm{Pr}^{2/3} - 1\right)}\left(\frac{k}{d_h}\right) \tag{14}$$

The pressure equation of the system needs to be used in order to evaluate the unknown mass flow rate, which is necessary to iteratively solve the analytic model is finally reported [16]:

$$p = H_{ch} \cdot \rho_a \beta_a g \left(T_f \left(r = r_i\right) - T_a\right) + \frac{\dot{m}^2 \rho_a \left(r_o^{-2} - r_i^{-2}\right)}{8 H_c^2 \pi^2 \rho_f^2} - \frac{\dot{m}^2}{A_c^2 \rho_{f,\,c}} \frac{c_F}{H_c} \left(r_o - r_i\right) + ... \\ ... - 2 \frac{\dot{m}^2}{A_{ch}^2 \rho_{f,\,ch}} \frac{H_{ch} c_F}{d_{ch}} - \frac{8}{27} \frac{\dot{m}^2}{A_T^2 \rho_{ch}} \tag{15}$$

The solution to this equations system allows reveals the temperature of SUPP components by varying the solar radiation. As reported by Sangi [16], for a solar flux of 1000$[W/m^2]$, the absorber temperature shows an average temperature of 70$[°C]$, while the internal roof surface increases up to about 50$[°C]$(Fig.6). These results were used in this paper as boundary conditions

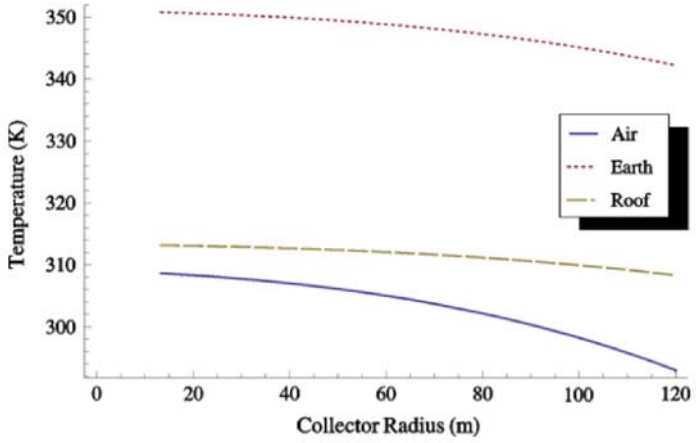

Figure 6: SUPP temperature trends @ q=1000 $[W/m^2]$.

for the numerical analysis, by setting fixed temperatures for the absorber surface and for the internal roof surface. The power of the SUPP is instead evaluated by scaling the available pressure obtained in the numerical simulation in absence of the turbine [5]:

$$x = \frac{\Delta p_{turb}}{\Delta p_{poten}} \tag{16}$$

$$P = \eta_{turb} \left(x \Delta p_{poten,\,no\,turb}\right) \left(\sqrt{1 - x} \cdot v_{inlet\,turb,\,no\,turb}\right) \tag{17}$$

The output power estimated using this scaling method, however, was recently found to be significantly lower than that calculated under a turbine load condition, based on the assumed x value of 0.8 [20].

4. Numerical Analysis

Numerical simulations were carried out by using the STAR-CCM+ commercial software with an Unsteady Reynolds-Averaged Navier-Stokes (URANS) approach. A summary of the selected options:

- A turbulent flow; i.e. the Rayleigh number for the collector dimensions and the temperature assumptions is largely greater than 10^8.
- A realizable $k - \epsilon$ turbulence model.

- Implicit with a first order temporal discretization.
- Air as ideal gas with compressible flow and a gravity model that allows the inclusion of the body force due to gravity in the momentum equations. In the full buoyancy model, the buoyancy force is evaluated directly from the difference between air density and a constant reference density though the compressibility factor for air is considered. Other authors [21] observed that neglecting air compressibility inside or outside the SUPP results in inaccuracy in the calculated results.
- Segregated approach for $p - u$ decoupling.

A 2D approach was selected for all simulations, thanks to the axial symmetry of the problem, except for the curved guide vanes analysis where a flow swirl is present and also a three-dimensional behavior is observed. By using a 2D model the overall number of mesh elements was reduced and so the computational effort. Polyhedral mesh was used for all domain extent (Fig.8) except

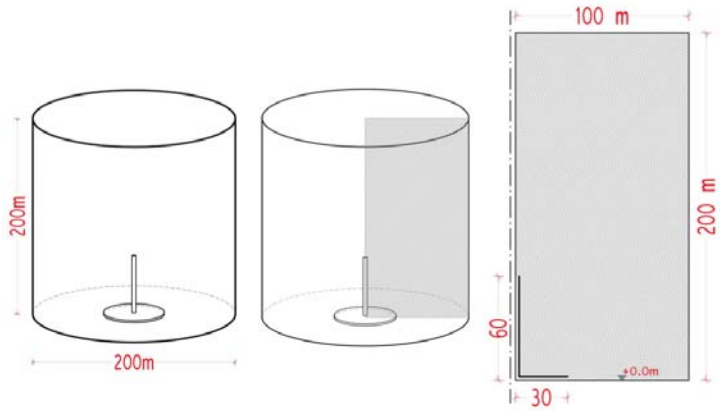

Figure 7: Computational domain.

near walls where 5 prism layers were selected with a stretch of 1.2 and a prism layer thickness of 0.3$[m]$; in this way and by selecting the two layer all y^+ wall treatment model, it was possible to obtain the values of the y^+ between 70 and 160 inside the SUPP. The CFD domain extends 3

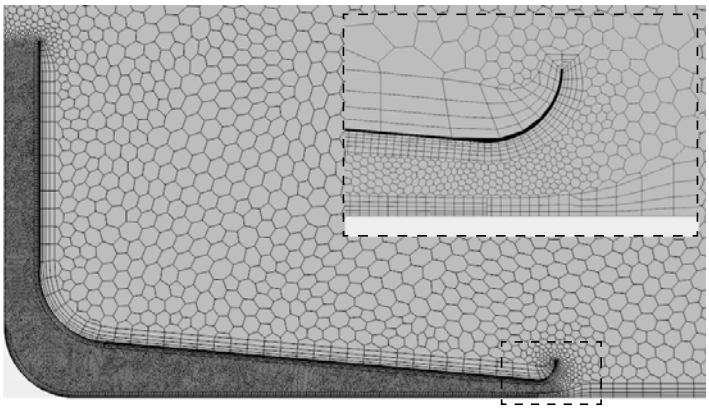

Figure 8: Adopted mesh.

times the SUPP characteristic length both in the vertical and horizontal directions; this distance between the external boundaries and the solar tower is large enough to ensure the development of an undisturbed flow pattern. The choice to include the outside domain by avoiding a boundary condition at the inlet and outlet of the SUPP derives from the results of previous analyses

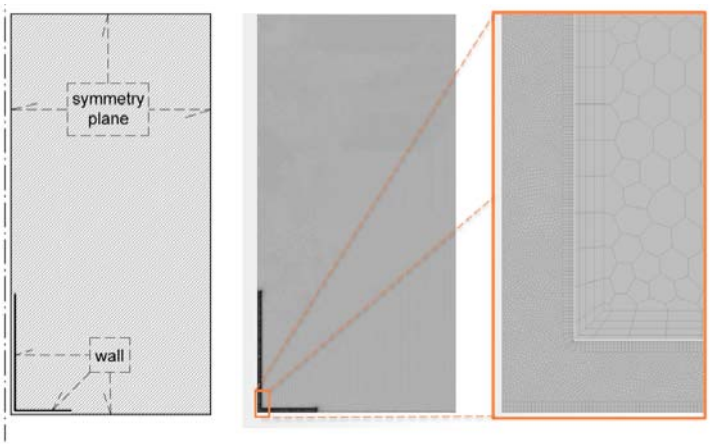

Figure 9: Bounday conditions.

of other authors that concluded it to be more realistic solar chimney inlet and outlet conditions [22].
As reported in table 1 several CFD analyses were carried out: i.e. six 2D models and one 3D model. Model 0 simulates the full scale Manzanares SUPP, while the others refer to the 1:2 scaled model prototype (Fig.10). Model 1 is a scaled version of the Manzanares plant so it has a flat roof and no corner fillet. Model 2 exhibits no round corners but a sloped roof, as suggested by several authors [15, 5]. Model 3 introduces aerodynamic optimization so as to reduce kinematic losses at the collector inlet, by using a bellmouth profile, and at the chimney section change, by rounding both the corner with the collector roof and the floor profile in the proximity of the plant central axis. Model 4 exhibits an additional change with a sloped floor that ensures a quasi-constant flow passage area and a small divergence to contrast the wall boundary layer development. Model 5 is designed as model 3, but with a lower chimney; i.e. $20[m]$ vs. $60[m]$. Finally, model 6 introduces, when compared to model 4, curved guide vanes so to induce a swirl motion. The numerical simulation for the model corresponding to the Manzanares prototype

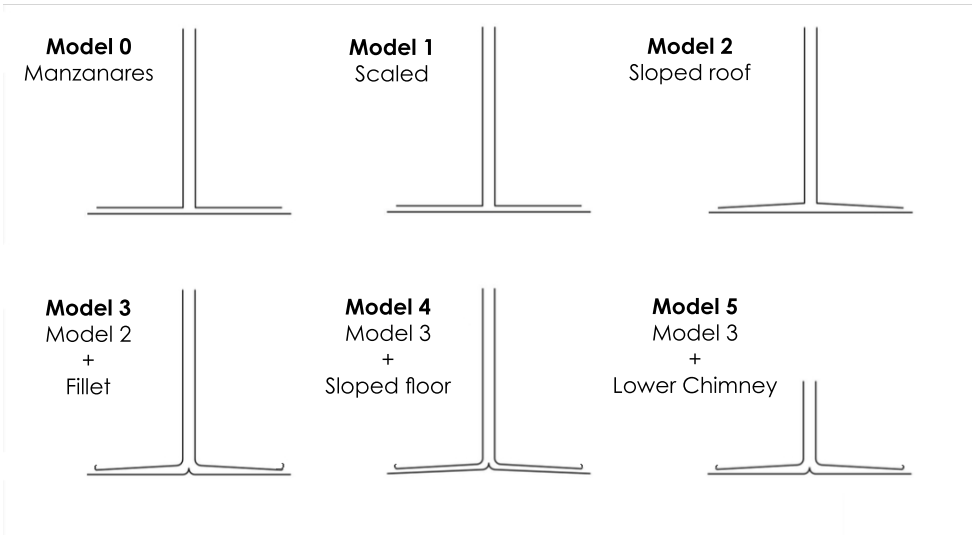

Figure 10: CFD Models.

(without turbine) shows a temperature increase of about 15 $[°C]$ and an updraft velocity of about 10 $[m/s]$ (Fig.12) with respect to real values (with turbine) of 7–9 $[m/s]$ (Fig.11) and a maximum collector temperature rise of 15–18 $[°C]$. It is so possible to affirm that there is a

Table 1: CFD models.

Name	Description	Used approach
Model 0	Manzanares SUPP	2D
Model 1	Scaled SUPP	2D
Model 2	Model 1 with roof sloped	2D
Model 3	Model 2 with shape optimization	2D
Model 4	Model 3 with floor sloped	2D
Model 5	Model 3 with lower chimney	2D
Model 6	Model 4 with curved vanes	3D

good correspondence for the CFD model because it was observed [17] that the turbine presence induces lower updraft velocities in the order of 2-3 $[m/s]$ and higher temperatures due to the lower flow velocity and longer exchange time in the collector. The comparison shows a good agreement also in terms of available power: Manzanares experimental data exhibit values ranging from 26.3 to 38.6$[kW]$ for a solar irradiation of 1000$[Wm^{-2}]$, while numerical CFD analyses show a potential value, estimated on the updraft velocity, of 26.2$[kW]$.

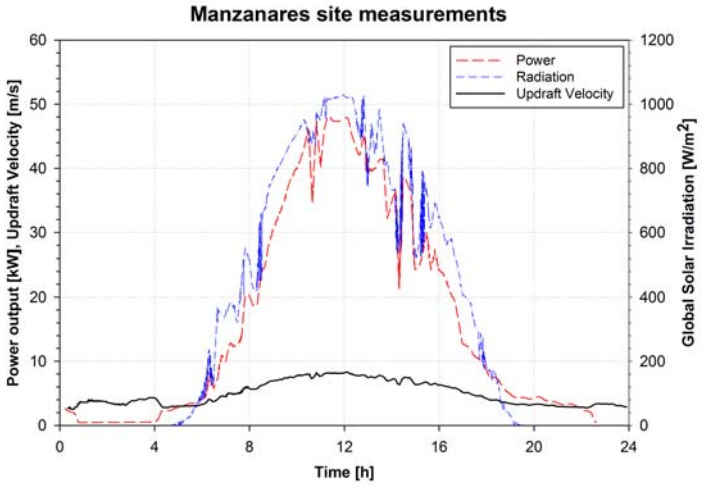

Figure 11: Manzanares measurements.

On this basis subsequent analyses were carried out with the same boundary conditions.

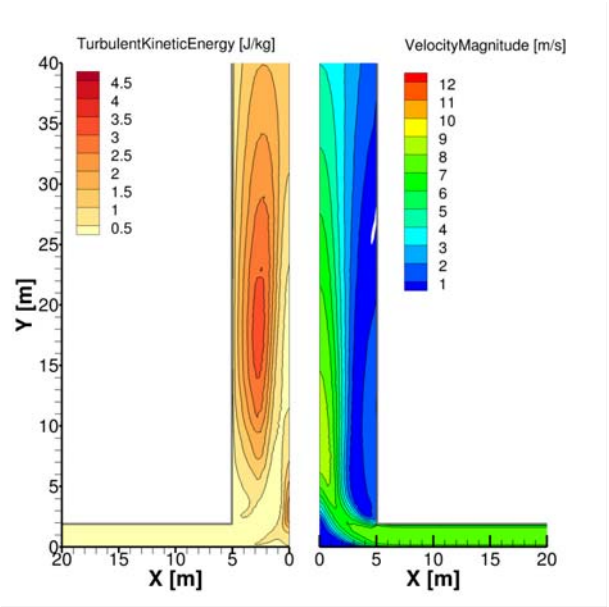

Figure 12: Model-0 Turbulent Kinetic Energy and Velocity Magnitude.

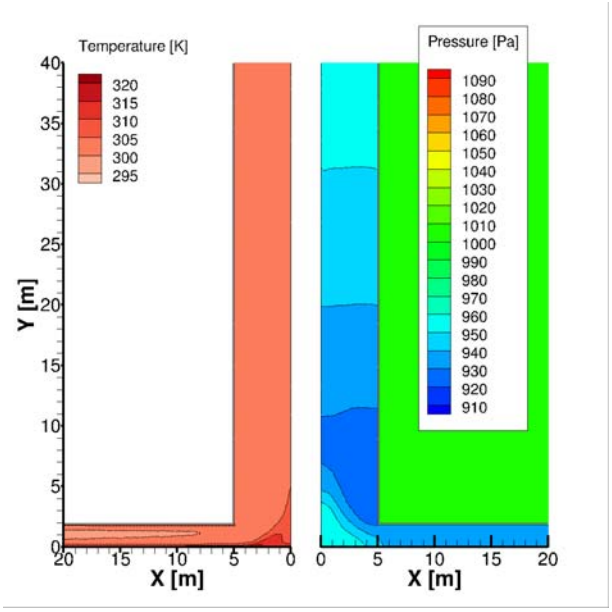

Figure 13: Model-0 Temperature and Relative pressure.

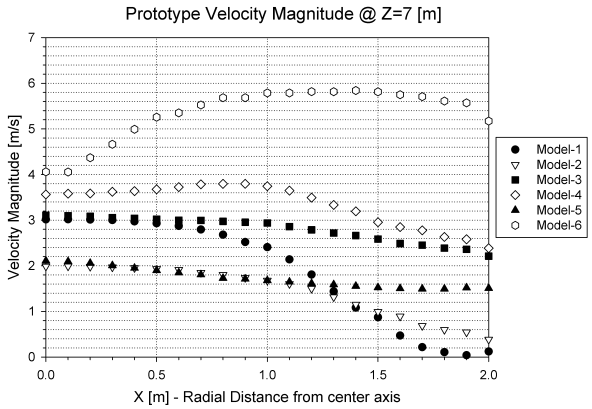

Figure 14: Velocity comparison @ Z=7 [m].

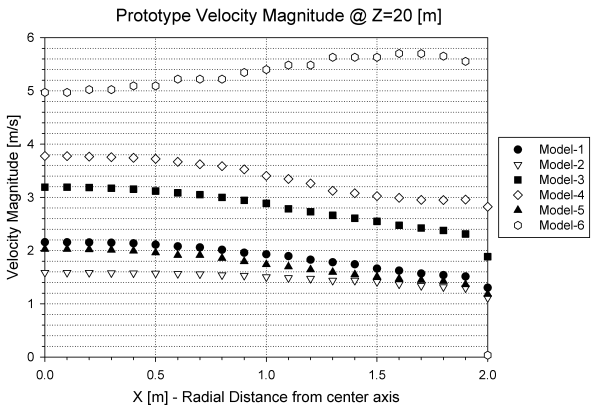

Figure 15: Velocity comparison @ Z=20 [m].

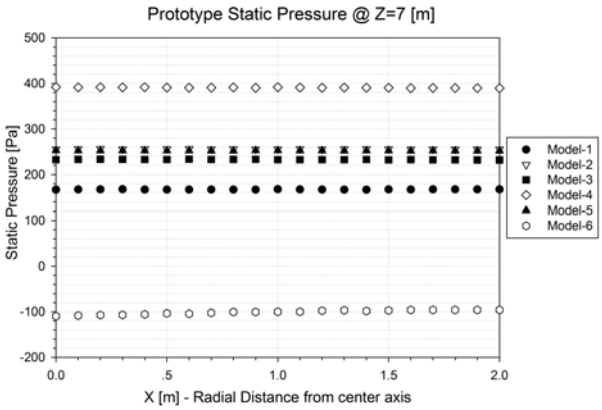

Figure 16: Static pressure comparison @ Z=7 [m].

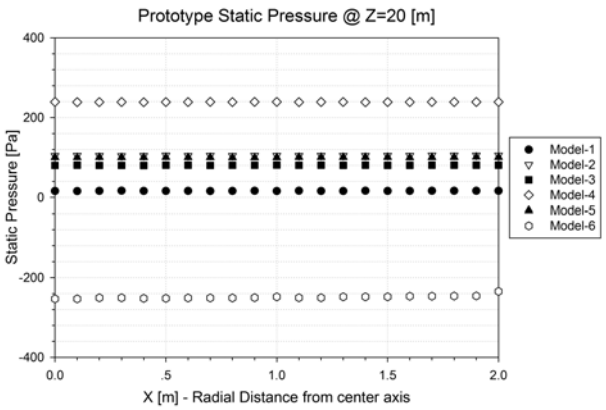

Figure 17: Static pressure comparison @ Z=20 [m].

Model 1 shows, as expected, a drastic reduction of SUPP performance parameters, with a maximum updraft velocity of about 3 $[m/s]$, a very low temperature increase and also lower pressure decrease to be used in the turbine energy production. A strong flow separation occurs around the corner between the collector roof and the chimney and a stagnation zone is instead present over the floor near the plant central axis.
Model 2 shows the worst behavior among the tested models, with lower velocities than model 1 and with a maximum updraft value of about $2[m/s]$; it however exhibits an higher temperature increase and also lower pressure decrease with respect to the model 1. The lower velocities can be associated to the flow expansion in the final section of the collector.
Model 3 shows better behavior than model 1, with a maximum updraft value of the same order (about 3 $[m/s]$), but with a more uniform velocity profile along the radius. It also shows higher temperatures and also lower pressure.
Model 4 has very good performance with maximum velocities of 3.8 $[m/s]$ and an almost uniform velocity distribution. This better performance is associated to the constant flow passage area that ensures a reduction of kinetic losses.
Model 5 has very poor performance that is comparable to model 2; this behavior is due to the lower chimney that does not promote the updraft natural convection.
Finally model 6 exhibits the best performance with velocities up to 5.8 $[m/s]$ and a radial distribution that shifts higher velocities to the outer radius. This behavior is related to the swirl motion and could be more useful for the turbine energy conversion developing higher torques. Also the figures 16 and 17 underline the observations reported by analyzing the radial distribution of the updraft velocities: the suggested adjustments show an improvement of the available pressure starting from the model 1 up to the model 4, with the exception of model 5 that behaves worse due to the Chimney's lower height. A completely different behavior is showed by the model 6 due to the pressure depression induced by the swirling flow, that increases the elaborated flow and substantially alters the SUPP's behavior.

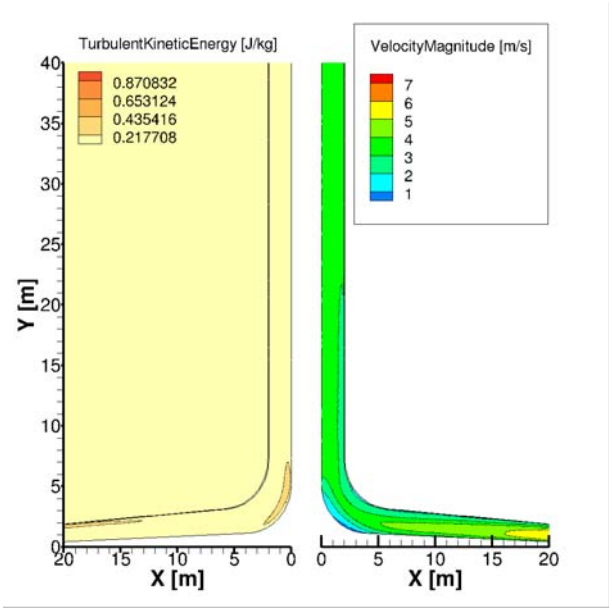

Figure 18: Model-4 Turbulent Kinetic Energy and Velocity Magnitude.

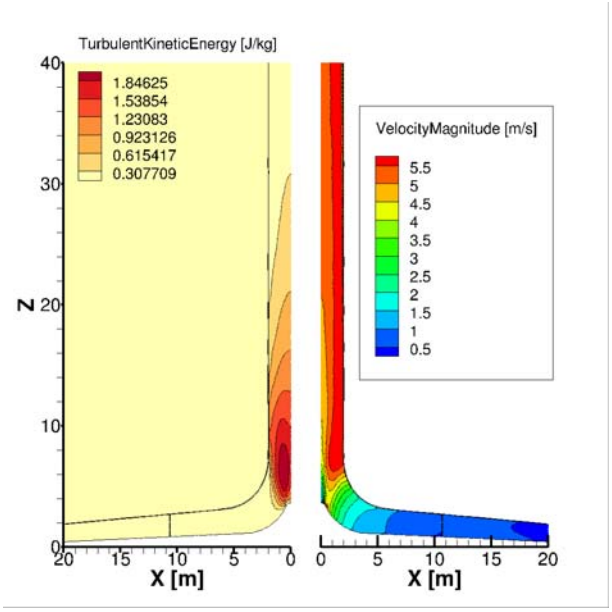

Figure 19: Model-6 Turbulent Kinetic Energy and Velocity Magnitude.

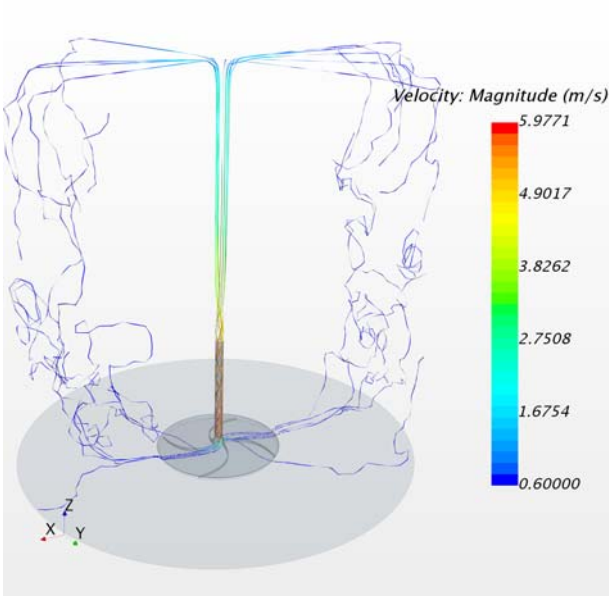

Figure 20: Model-6 Flow pattern.

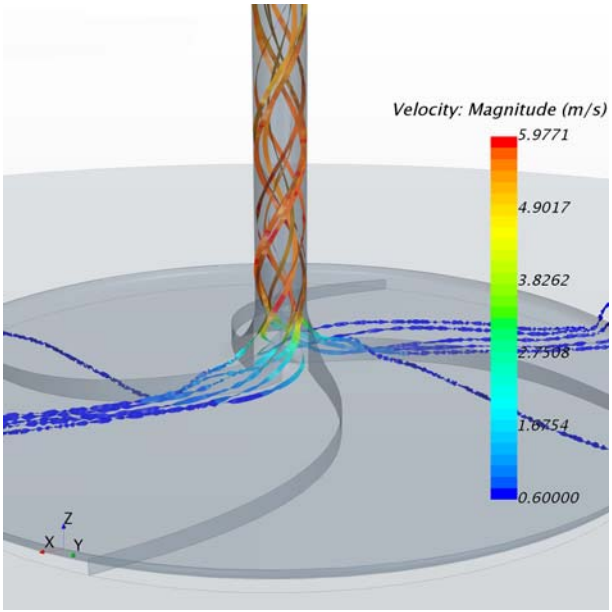

Figure 21: Model-6 Flow swirl.

5. Conclusions

This paper is aimed to numerically analyze the behavior of a SUPP scaled prototype. Once analyzed, the analytic model defined the boundary conditions for the subsequent numerical simulations. Several models were tested: initially a model 0 corresponding to the Manzanares experimental setup was computed in order to verify the correctness of the used approach. Following that, other configurations were tested so as to identify the best solutions; these

correspond to sloped roof and floor, to a bellmouth profile at the collector inlet, and to the use of curved vanes able to induce swirl.

6. Nomenclature

Pr	Prandtl number
Ra	Rayleigh number
Re	Reynolds number
η	Efficiency
β	Volumetric expansion coefficient
ρ	Density $[\frac{kg}{m^3}]$
σ	Stephan-Boltzmann constant $[\frac{W}{m^2K^4}]$
τ	Radiative trasmissivity coefficient
ε	Radiative emissivity
$_a$	Ambient
$_f$	Flow
$_i$	Inner
$_o$	Outer
$_{ch}$	Chimney
is	Isoentropic
$\dot{m}$	Mass flow rate $[\frac{kg}{s}]$
$\dot{Q}$	Heat flux $[W]$
$\dot{W}'$	Mechanical Power $[W]$
A_c	Collector cross sectional area $[m^2]$
A_ch	Chimney cross sectional area $[m^2]$
A_T	Turbine cross sectional area $[m^2]$
g	Gravitational acceleration $[\frac{m}{s^2}]$
h	Enthalpy $[\frac{J}{kg}]$
H_{ch}	Chimney height $[m]$
p	Pressure $[Pa]$
T	Temperature $[°C]$
v	Velocity $[\frac{m}{s}]$
z	Geodetical height $[m]$
c_p	Specfic Heat $[\frac{J}{kgK}]$
f	Friction coefficient
h_c	Convective heat transfer coefficient $[\frac{W}{m^2K}]$
h_k	Conductive heat transfer coefficient $[\frac{W}{m^2K}]$
h_r	Radiative heat transfer coefficient $[\frac{W}{m^2K}]$
r	Collector radius $[m]$
S_P	Floor absorbed solar radiation $[\frac{W}{m^2}]$
S_R	Roof absorbed solar radiation $[\frac{W}{m^2}]$
$\dot{q}_{solar}$	Solar irradiation $[\frac{W}{m^2}]$

References

[1] Haaf W, Friedrich K, Mayr G and Schlaich J 1983 *Int. J. Solar Energy* **2** 3–20
[2] Haaf W 1984 *Int. J. Solar Energy* **2** 141–161 ISSN 0142-5919
[3] Schlaich J 1995 *The Solar Chimney: Electricity From the Sun.* (Edition Axel Menges)
[4] Zhou X, Wang F and Ochieng R M 2010 *Renewable Sustainable Energy Rev.* **14** 2315–2338 ISSN 13640321
[5] Zhou X and Xu Y 2016 *Sol. Energy* **128** 95–125 ISSN 0038092X
[6] Dhahri A and Omri A 2013 *Int. J. Eng. Adv. Technol.* **2** 2249–8958
[7] Al-Kayiem H H and Aja O C 2016 *Renewable Sustainable Energy Rev.* **58** 1269–1292 ISSN 13640321
[8] PASUMARTHI N and SHERIF S A 1998 *Int. J. Energy Res.* **22** 443—461
[9] PASUMARTHI N and SHERIF S A 1998 *Int. J. Energy Res.* **22** 277—288
[10] Gannon A J and von Backström T W 2000 *J. Sol. Energy Eng.* **122** 133 ISSN 01996231
[11] dos S Bernardes M, Voß A and Weinrebe G 2003 *Sol. Energy* **75** 511–524 ISSN 0038092X
[12] Pretorius J and Kröger D 2006 *Sol. Energy* **80** 535–544 ISSN 0038092X
[13] von Backström T and Gannon A 2004 *Solar Energy* **76** 235–241 ISSN 0038092X
[14] Schlaich J, Bergermann R, Schiel W and Weinrebe G 2005 *J. Sol. Energy Eng.* **127** 117–124
[15] Cottam P, Duffour P, Lindstrand P and Fromme P 2016 *Sol. Energy* **129** 286–296 ISSN 0038092X
[16] Sangi R, Amidpour M and Hosseinizadeh B 2011 *Sol. Energy* **85** 829–838 ISSN 0038092X
[17] Fasel H F, Meng F, Shams E and Gross A 2013 *Sol. Energy* **98** 12–22 ISSN 0038092X
[18] Koonsrisuk A and Chitsomboon T 2013 *Energy* **51** 400–406 ISSN 03605442
[19] Choi Y J, Kam D H, Park Y W and Jeong Y H 2016 *Energy* **112** 200–207 ISSN 03605442

[20] Zhou X, Yuan S and Bernardes M A d S 2013 *Int. J. Heat Mass Transfer* **66** 798–807 ISSN 00179310
[21] Zhou X, Yang J, Xiao B, Hou G and Xing F 2009 *Appl. Therm. Eng.* **29** 178–185 ISSN 13594311
[22] Shams E, Gross A and Fasel H 2011 *Performance analysis of solar chimneys of different physical scales using CFD* parts a, b, and c ed ISBN 9780791854686